JOURNAL OF MATERIALS SCIENCE **38** (2003) 727–737

V^{4+} in quenched calcium silicates: An electron spin resonance spectroscopic investigation

H. FARAH*
Department of Mechanical and Industrial Engineering, Concordia University, Montreal, QC H3G 1M8, Canada
E-mail: farah_1@me.concordia.ca

Electron spin resonance (ESR) studies of vanadium(IV) have been carried out on CaO-SiO_2, CaO-MgO-SiO_2 and CaO-Al_2O_3-SiO_2 slags equilibrated with oxygen partial pressures over the range 10^{-9}–10^{-2} atm and also CaO-SiO_2-V_2O_5-Fe_2O_3 slag melted in air. The slags were melted at 1873 K and their V_2O_5 level was varied between 1 and 10 mol%. Three different melt basicities and alumina contents were investigated. Magnesia content was varied between 3.5 and 4.9 wt%. An industrial slag sample was also examined. The spin Hamiltonian parameters were determined and it was concluded that the paramagnetic vanadium was in the form of a distorted octahedral vanadyl complex (VO^{2+}). An overlapping signal from a yet unknown paramagnetic vanadium species was present in all slags. In general this signal diminished with reduction in the oxygen pressures below 10^{-6} atm and V_2O_5 content. It also decreased with increase in basicity and magnesia content. The critical fraction of paramagnetic vanadium for induction of the second species was dependent on melt composition.

1. Introduction

The V^{4+} ion, being paramagnetic in nature, produces a characteristic eight line ESR spectrum. In the various germinate, phosphate, borate [1], sodium [2, 3] and alumina [4] silicate and tellurite [5, 6] glasses studied, V^{4+} has been found as a tetragonally distorted octahedral $(VO)^{2+}$ complex which tends to become less distorted from octahedral symmetry with an increase in the basicity of the medium. There are a few cases [3, 4, 7] in which V^{4+} was fund to be coordinated at tetrahedral sites. Generally it is difficult to resolve the V^{4+} spectrum as its concentration, or the total vanadium content increased [6, 8] and when this happens it is difficult to calculate the g-values. The existence of VO^{2+} ion has also been confirmed in phosphate glasses using chromatographic analysis [9].

Another ESR study made by Farah *et al.* [8] has revealed V^{4+} coordination in quenched sodium silicate melts in detail. The present work is the continuation of the same project and it aims to examine the V^{4+} in calcium silicate and complex metallurgical slags, since there has been no indication of such work in literature and it is important to understand the coordination of vanadium in these slags.

2. Experimental procedure

50 g of master melts were prepared from analytical grade CaO, MgO, Al_2O_3, SiO_2 and V_2O_5. All reagents were dried at 393 K for 24 hours, then carefully weighed and mixed. These were melted in a platinum crucible at 1873 K, crushed in a tungsten mill and analysed by XRF. Compositions and identifications of the slags are given in Table I. Equilibration time was determined in a separate kinetic study.

A molybdenum wound electric resistance tube furnace was used for the equilibrium experiments. The temperature of the furnace was controlled by a Eurotherm temperature controller (±5 K). 1–2 g of samples were placed in platinum crucible and equilibrated at 1873 K in air and over a range of oxygen partial pressures (10^{-2}–10^{-9} atm). The samples were then quenched in the bottom water-cooled quenching chamber in the same gaseous atmosphere. Ar, CO, CO_2 and Ar-O_2 gas mixtures were used for the preparation of various compositions using a precalibrated mass flow controller.

A Varian E-line spectrometer operating in X band at 9.48 GHz was used for the analysis of vanadium(IV). All spectra were recorded over 2000G at room temperature on quenched slags. Details of the ESR analysis are given elsewhere [8]. The ESR spectrum was recorded for the industrial slag sample from New Zealand Steel. Its composition is given with Table I.

XPS spectra were measured on a KRATOS (XSAM 800 pci) spectometer using Mg K_α X-rays on thin films of samples ($\leq$1 mm) of slag C. Argon ion etching was used to obtain information on composition of the slag.

*Author to whom all correspondence should be addressed.

TABLE I Details of composition of slag samples

S. no.	CaO/SiO_2 (molar ratio)	V_2O_5 (mol%)	MgO (wt%)	Al_2O_3 (wt%)	Fe_2O_3 (mol%)
A	0.7	5	–	–	–
B	0.9	5	–	–	–
C	1.23	5	–	–	–
D	0.7	1	–	–	–
E	0.9	1	–	–	–
F	1.21	3	–	–	–
G	1.57	5	3.50	–	–
H	1.51	5	4.87	–	–
I	1.23	5	–	3.22	–
J	1.22	5	–	5.44	–
K	1.22	5	–	7.87	–
L	1.25	10	–	–	10
M	1.56	10	–	–	10

The composition (wt%) of slag sample from New Zealand Steel: Fe(tot) = 12.72, CaO = 51.41, SiO_2 = 9.85, Al_2O_3 = 2.35, MgO = 8.77, V_2O_3 = 4.11, TiO_2 = 3.72, Cr_2O_3 = 0.324, MnO = 2.16, P_2O_5 = 1.365 and S = 0.185.

3. Results

V^{4+} in the form of tetragonally distorted octahedral VO^{2+} ion exhibited a characteristic spectrum at room temperature, featuring a spin Hamiltonian function as [10]:

$$H = g_{II}\beta S_z H_z + g_\perp \beta (S_x H_x + S_y H_y) + A_{II} S_z I_z + A_\perp (S_x I_x + S_y I_y) \quad (1)$$

where β is the Bohr magneton, g_{II} and $g_\perp$, the parallel and perpendicular components of the g-tensor and A_{II}, and $A_\perp$ are the parallel and perpendicular components of hyperfine tensor; H_x, H_y and H_z are the components of the magnetic field; I_x, I_y and I_z and S_x, S_y and S_z are the components of the nuclear and electron spin operators respectively.

The absorption signal can be described as a set of envelopes [1], one for each of the $2I + 1$ values of m. For each of the envelopes, the resonant magnetic field strengths for spins parallel and perpendicular to the axial direction are given respectively by:

$$H_{II} = 2H_o/g_{II} - (A_{II}/g_{II}\beta)m \quad \text{for } \theta = 0 \quad (2)$$

and

$$H_\perp = 2H_o/g_\perp - (A_\perp/g_\perp\beta)m \quad \text{for } \theta = \pi/2 \quad (3)$$

where H_o is the center field and m, the nuclear magnetic quantum number. As mentioned previously [8], the following equations were used in order to determine the degree of covalent bonding:

$$A_{II} = -P[\beta^2(4/7 + K) + \Delta g_{II} + 3/7\Delta g_\perp] \quad (4)$$

and

$$A_\perp = P[\beta^2(2/7 - K) - 11/14\Delta g_\perp] \quad (5)$$

where β^2 is the measure of the degree of π bonding and is unity for a purely ionic bond. $\Delta g_{II} = 2.0023 - g_{II}$ and $\Delta g_\perp = 2.0023 - g_\perp \cdot \Delta g_{II}/\Delta g_\perp$ could be used to

TABLE II g's and A's for various quenched vanadium silicates

Sample no.	V_{PAR}	g_{II} (±0.001)	$g_\perp$ (±0.001)	$A_{II} \times (10^{-4}$/cm,[a] ±0.5)	$A_\perp \times (10^{-4}$/cm,[a] ±0.5)
A 1	–	1.932	1.980	163.6	64.7
2	–	1.933	–	164.3	–
3	–	1.936	–	162.5	–
4	–	1.935	1.980	164.2	64.6
5	–	1.922	1.965	162.8	62.2
B 1	0.433	1.923	1.969	162.1	64.6
2	0.691	1.923	1.965	161.8	62.2
3	0.653	1.923	1.965	160.9	62.2
4	0.264	1.924	1.965	162.0	62.2
5	0.151	1.922	1.965	162.8	62.2
C 1	0.364	1.922	1.969	162.7	64.7
2	0.628	1.924	1.965	160.2	61.7
3	0.591	1.927	1.963	160.0	62.2
4	0.377	1.923	1.965	161.6	60.6
5	0.251	1.923	1.964	161.8	60.6
C a	0.369	1.929	1.973	162.8	63.0
b	0.282	1.928	1.978	164.3	64.7
c	0.266	1.928	1.975	162.7	63.0
d	0.273	1.929	1.975	163.3	62.0
e	0.254	1.929	1.975	163.0	63.6
f	0.268	1.929	1.974	162.0	62.2
D 1	–	1.928	1.976	165.1	62.5
2	–	1.929	1.979	164.5	64.4
3	–	1.930	1.978	163.5	64.6
4	–	1.930	1.977	165.3	64.6
5	–	1.929	1.974	164.5	60.6
E 1	–	1.929	1.976	164.2	62.2
2	–	1.929	1.978	163.1	64.6
3	–	1.929	1.978	163.1	64.7
4	–	1.929	1.978	163.1	64.7
5	–	1.929	1.974	164.5	60.6
F 1	0.501	1.933	1.979	163.8	62.2
2	0.602	1.934	1.978	163.2	63.0
3	0.662	1.935	1.980	161.8	61.4
4	0.582	1.936	1.979	161.3	62.2
5	0.401	1.934	1.976	162.4	59.8
G 1	0.123	1.932	1.976	161.5	60.4
2	0.308	1.933	1.977	161.5	60.6
3	0.441	1.934	1.978	161.0	63.0
H 1	0.097	1.933	1.977	161.5	59.8
2	0.257	1.934	1.979	161.5	62.2
3	0.394	1.936	1.980	160.5	64.0
H a	0.098	1.929	1.974	160.0	62.2
b	0.091	1.930	1.972	161.9	60.6
c	0.090	1.926	1.974	161.1	60.2
d	0.085	1.930	1.974	159.5	61.4
e	0.090	1.927	1.972	161.9	59.8
I 1	0.287	1.922	1.969	162.7	64.7
2	0.615	1.936	1.979	162.1	60.6
3	0.574	1.941	1.979	159.3	60.6
4	0.400	1.941	1.978	160.3	59.8
5	0.328	1.940	1.981	160.5	60.3
J 1	0.308	1.936	1.980	163.1	62.2
2	0.627	1.938	1.980	161.7	61.4
3	0.590	1.942	1.980	159.9	60.3
4	0.357	1.940	1.979	159.8	60.6
5	0.234	1.939	1.979	160.0	59.3
K 1	0.365	1.934	1.979	161.9	61.4
2	0.559	1.939	1.979	159.4	62.2
3	0.491	1.937	1.978	159.5	63.0
4	0.326	1.931	1.981	161.3	62.2
5	0.195	1.936	1.978	161.5	61.2

[a]Negative.

Upper case alphabets A–K represent slag names (from Table I), 1–5 represent oxygen partial pressures (pO_2) 10^{-2}, 10^{-4}, 10^{-6}, 10^{-8} and 10^{-9} atm and a–f represent 1–6 hours of equilibration at the given oxygen potential.

TABLE III $\Delta g_{II}/\Delta g_{\perp}$ for different slag samples

Sample no.	$\Delta g_{II}/\Delta g_{\perp}$ (±0.002)	Sample colour	Sample no.	$\Delta g_{II}/\Delta g_{\perp}$ (±0.002)	Sample colour
A 1	3.203	Light brown	F 2	2.777	Light brown
4	3.049	Dark brown	3	2.974	Dark brown
5	2.128	Dark brown	4	2.815	Brown
B 1	2.365	Light brown	5	2.598	Brown
2	2.148	Dark brown	G 1	2.661	Beige
3	2.036	Dark brown	2	2.689	Light brown
4	2.076	Dark brown	3	2.828	Brown
5	2.128	Dark brown	H 1	2.733	Beige
C 1	2.397	Light brown	2	2.895	Brown
2	2.085	Brown	3	2.912	Dark brown
3	2.024	Brown	H a	2.574	–
4	2.001	Brown	b	2.373	–
5	2.097	Light brown	c	2.661	–
C a	2.499	–	d	2.586	–
b	3.046	–	e	2.530	–
c	2.743	–	I 1	2.397	Light brown
d	2.661	–	2	2.829	Brown
e	2.707	–	3	2.829	Brown
f	2.569	–	4	2.539	Brown
D 1	2.828	White	5	2.871	Brown
2	3.126	Beige	J 1	2.942	Light brown
3	2.985	Beige	2	2.901	Brown
4	2.898	Beige	3	2.768	Dark brown
5	2.545	White	4	2.686	Dark brown
E 1	2.820	White	5	2.726	Dark brown
2	3.015	Light brown	K 1	2.945	Light brown
3	3.015	Light brown	2	2.667	Brown
4	2.968	Light brown	3	2.651	Dark brown
5	2.545	White	4	3.364	Dark brown
F 1	2.943	Beige	5	2.779	Dark brown

determine the degree of tetragonal distortion of the vanadyl complex. $P\beta^2K$ is a measure of s character of the spin of the vanadium and also the tetragonal distortion, where K is the Fermi contact interaction term and P is the dipolar hyperfine coupling parameter. The values of g_{II}, $g_{\perp}$, A_{II}, $A_{\perp}$, P, $P\beta^2K$ and $\Delta g_{II}/\Delta g_{\perp}$ obtained using Equations 1–5 according to the method described earlier [8]. g_{II}, $g_{\perp}$, A_{II}, $A_{\perp}$ and $\Delta g_{II}/\Delta g_{\perp}$ are given in Tables II and III for different samples. These results are consistent with the previous studies in related quenched melts [1, 2]. It was difficult to determine the perpendicular components in the spectra due to the overlapping signals from the second form of V^{4+} and poor resolution due to larger line widths. The trends in the degree of distortion of the octahedral symmetry determined from the bonding parameters may be affected by vanadium volatilization under reduced oxygen pressures.

3.1. $CaO\text{-}SiO_2\text{-}V_2O_5$ melt

This system was studied to find the ESR patterns of V^{4+} in slags with different basicity ratios and V_2O_5 content over the range of oxygen partial pressures 10^{-2}–10^{-9} atm. The effect of variation in melting time was also studied.

Fig. 1 presents the V^{4+} spectra measured at room temperature for $CaO\text{-}SiO_2\text{-}V_2O_5$ prepared with 5 mol% V_2O_5 at three different basicity ratios ($CaO/SiO_2 = 0.7$, 0.9, 1.23) over the given pO_2 range (from a to e). It is obvious from the sequences 1, 2, 3 in Fig. 1 that the spectra are same as found earlier [8] and V^{4+} is present as a distorted octahedral VO^{2+} ion. the VO^{2+} spectrum is dominant at $pO_2 = 10^{-2}$ and 10^{-9} atm for each basicity ratio but at oxygen partial pressure between 10^{-4}–10^{-8} atm the additional broad signal coming

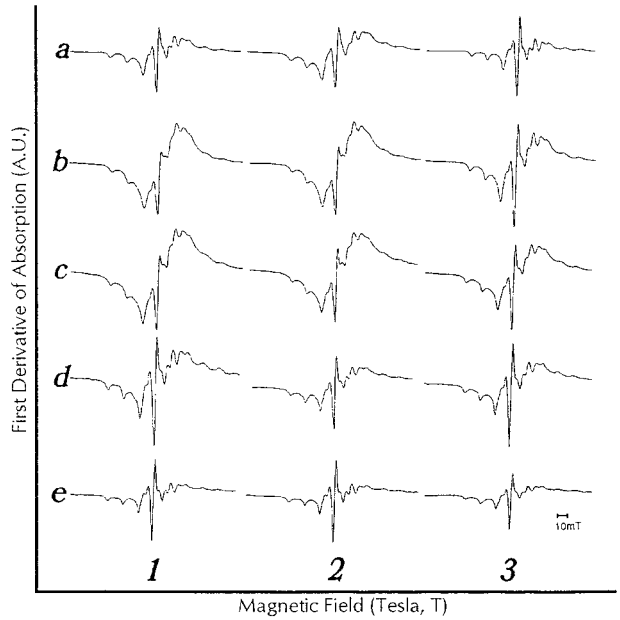

Figure 1 V^{4+} ESR spectra for quenched samples ($CaO\text{-}SiO_2\text{-}V_2O_5$ system) (1) A1–A5 $CaO/SiO_2 = 0.7$; (2) B1–B5 $CaO/SiO_2 = 0.9$; (3) C1–C5 $CaO/SiO_2 = 1.23$ (1600°C); (1–5 in Table II is labelled a–e here). See Tables I and II for details.

from the second form of V^{4+} is present. Increasing basicity from 0.7 to 1.23 apparently diminishes this broad signal within this range of oxygen pressures although its effect is not pronounced as some overlap still remained. These spectra also present poor resolution in addition to the overlap of the two signals.

It should be noted here that slag A, highly acidic in nature, had the same equilibration time as the other slags. Because of its acidic nature it may require longer equilibration time than other slags (C, F etc.) [8]. Therefore the fraction of paramagnetic vanadium (V_{PAR}) is not given for slag A (basicity ratio = 0.7), as it may not represent an equilibrium value. As the basicity ratio was increased to 0.9 (slag B), the V_{PAR} increased (Table II) from 10^{-2} till 10^{-4} atm and then it started to decrease. The fractions at 10^{-8} and 10^{-9} atm have been corrected for vanadium loss at 1873 K. The apparent reduction in the overlapping signal may be attributed to evaporation of vanadium (e.g. Fig. 1 sequence 1). However, it has been reported earlier [11] the reducing oxygen atmospheres have decreased the V^{4+} concentration in similiar melts. From the chemical analysis of the vanadium species [8] it was found that only V^{4+}/V^{5+} ionic pair was present at 10^{-2} atm while V^{3+}/V^{4+} pair between 10^{-6}–10^{-9} atm and two redox pairs coexisted at 10^{-4} atm.

With a further increase in basicity ratio to 1.23 for slag C, again the V_{PAR} increased from 10^{-2} till 10^{-4} atm and then it started to decrease. V_{PAR} remained lower at this basicity (1.23) compared to those at 0.9 (slag B) over the oxygen pressures range between 10^{-2}–10^{-6} atm. However no critical fraction for the induction of the second form of paramagnetic vanadium can be clearly defined since it varied with the melt composition. Relative to slag B, the oxygen partial pressure region for the coexistence of the two redox pairs was extended between 10^{-4} and 10^{-6} atm. Only V^{4+}/V^{5+} ionic pair was present at 10^{-2} atm and only V^{3+}/V^{4+} pair between 10^{-8}–10^{-9} atm.

$\Delta g_{II}/\Delta g_{\perp}$ ratios are plotted as a function of oxygen pressures in logarithmic scale at different basicity ratios for slag A, B and C in Fig. 2a. It shows that these ratios decrease with increase in basicity from 0.7 to 0.9 but are nearly same with a further increase to 1.23. Also the $\Delta g_{II}/\Delta g_{\perp}$ ratios remained lower as oxygen pressure was reduced. These results agree with our previous observation [8] and those of other researchers [1, 2] that octahedral symmetry is favoured with the increase in basicity of the slag. P and $P\beta^2K$ versus oxygen pressures plots at different basicity ratios are presented in Fig. 2b and c which indicate a decrease in P and $P\beta^2K$ values with increase in basicity from 0.7 (slag A) to 0.9 (slag B) and 1.23 (slag C) due to decrease in tetragonal nature of vanadyl ion which is in accord with the work on sodium silicates [8].

As indicated in sequences 1 and 2 in Fig. 3, V^{4+} exhibited well-resolved spectra with 1 mol% V_2O_5 at a basicity of 0.7 (slag D) and 0.9 (slag E). The additional broad signal from the second form of vanadium(IV) was present in the spectra of both slags. When the V_2O_5 content (slag F) was increased to 3 mol%, the overlapping signal was reduced, hyperfine splitting was restored and a better resolution was also achieved as is apparent in Fig. 3 sequence 3. But this may be attributed to higher basicity of slag F ($CaO/SiO_2 = 1.21$) relative to slags D & E ($CaO/SiO_2 = 0.7$ and 0.9 respectively), hence supporting the previous observation regarding the effect of basicity. However a comparison between slag C ($V_2O_5 = 5$ mol%, Fig. 1 sequence 3) and slag F ($V_2O_5 = 3$ mol%, Fig. 3 sequence 3), at the similar basicity ~1.2 indicates that the second form of V^{4+} is more pronounced at the highest content of V_2O_5, namely 5 mol% which agrees with our work on sodium silicates [8]. It was difficult to measure the g values for all these spectra, particularly the perpendicular component due to the additional broad signal.

It should be noted here as well that although slags D and E have acidic composition, these were equilibrated for the same time used for rest of the slags. Therefore fraction of paramagnetic vanadium (V_{PAR}) is not given for slags D and E as mentioned earlier for slag A. For slag F, only V^{4+}/V^{5+} ion pair was found at oxygen potential between 10^{-2}–10^{-4} atm and only V^{3+}/V^{4+} pair between 10^{-8}–10^{-9} atm with an overlap of two pairs at 10^{-6} atm [8].

$\Delta g_{II}/\Delta g_{\perp}$ ratios as a function of oxygen pressures in logarithmic scale for slags D–F are compared with slags A–C at similar basicity ratios at various V_2O_5 contents in Fig. 4a. It indicates that these ratios are higher for slag E (1 mol% V_2O_5) than slag B (5 mol% V_2O_5) and for slag F (3 mol% V_2O_5) than slag C (5 mol% V_2O_5). The decrease in $\Delta g_{II}/\Delta g_{\perp}$ ratios for V_2O_5 content between 1 to 5 mol% indicates that V_2O_5 content investigated is low compared to that found from previous work (i.e. in excess of 5 mol%) [5, 8], to reduce octahedral symmetry of $(VO)^{2+}$ complex. As discussed earlier, these ratios decreased at reduced oxygen pressure. A comparison of P and $P\beta^2K$ versus oxygen pressures plots at different V_2O_5 contents also show a decrease in P and $P\beta^2K$ values with increase in V_2O_5 from 1 to 5 mol% (Fig. 4b and c). This implies that the range of V_2O_5 content investigated is quite low compared to that found to be required (>5 mol%), from previous work [5, 8], to increase the covalent character and/or tetragonal distortion of the VO^{2+} complex. The trends in $\Delta g_{II}/\Delta g_{\perp}$, P and $P\beta^2K$ values are not clear from a comparison of slags D and A.

The V^{4+} spectra for samples (slag C) equilibrated with an Ar-O_2(2%) gas mixture between 1–6 hours are given in Fig. 5 sequence 1. It indicates that these are similar to each other except the intensity, which is higher for one and two hours. The slag generally needed greater than four hours to achieve equilibrium. $\Delta g_{II}/\Delta g_{\perp}$, P and $P\beta^2K$ for slag C do not indicate clear trends as a function of melting time (Table III).

3.2. CaO-MgO-SiO_2-V_2O_5 melt

Two different magnesium oxide contents were added to the base system at a basicity of about 1.5 and samples were prepared over the same oxygen potential range as mentioned earlier. As shown in Fig. 6 sequence 1, the addition of 3.5 wt% magnesia in slag G has reduced

the overlapping broad signal compared to MgO free $CaO\text{-}SiO_2\text{-}V_2O_5$ slag C (Fig. 1 sequence 3) at a similar basicity ratio and V_2O_5 content. The resolution of spectra was restored between $pO_2 = 10^{-2}$ to 10^{-4} atm. The signal started to broaden from $pO_2 = 10^{-6}$ atm and in addition there was the overlapping signal which made it difficult to measure the g values for the reduced oxygen pressures. A further increase of magnesia to 4.87 wt% (slag H) did not produce any obvious changes in the appearance of the spectra (Fig. 6 sequence 2) compared to slag G (Fig. 6 sequence 1) but the fraction of paramagnetic vanadium was reduced at this magnesia content as indicated in Table II over the given range of oxygen pressures. For slags G and H, the V^{4+}/V^{5+} ion pair was

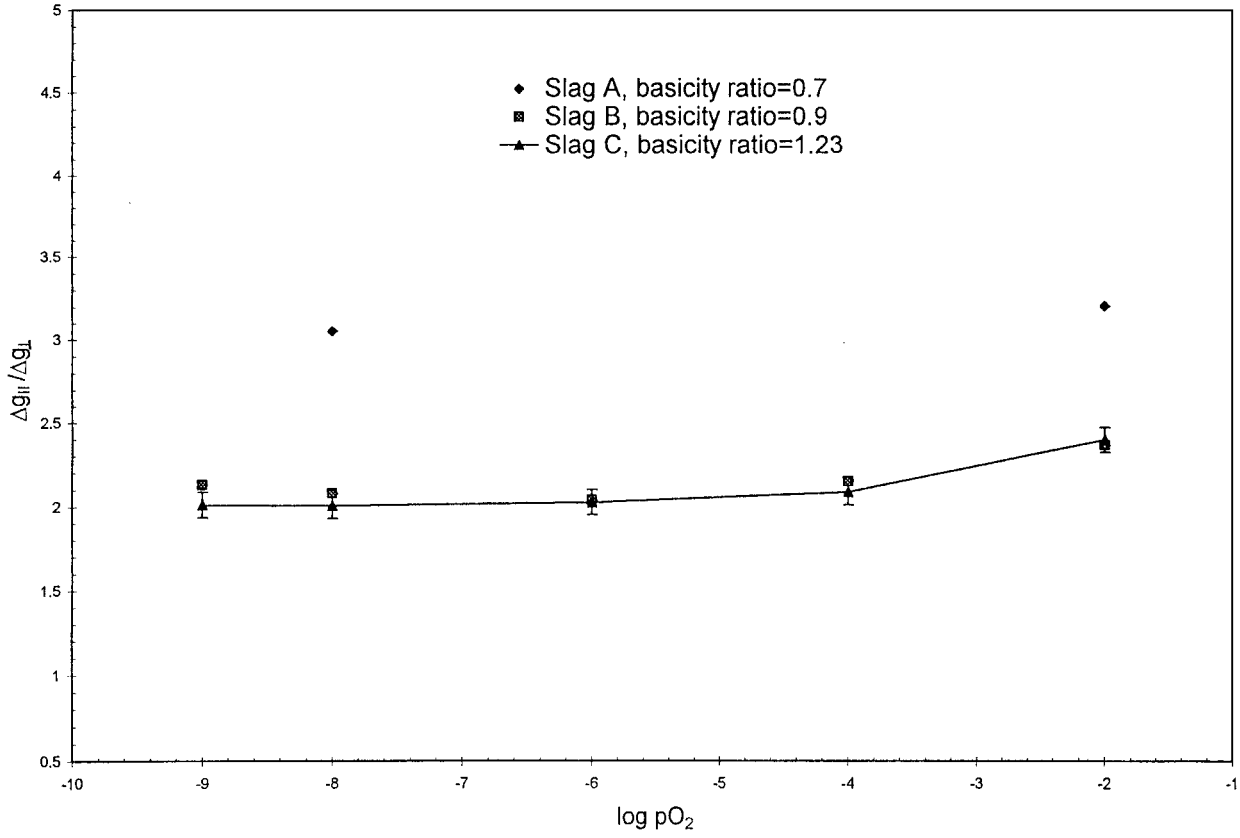

(a)

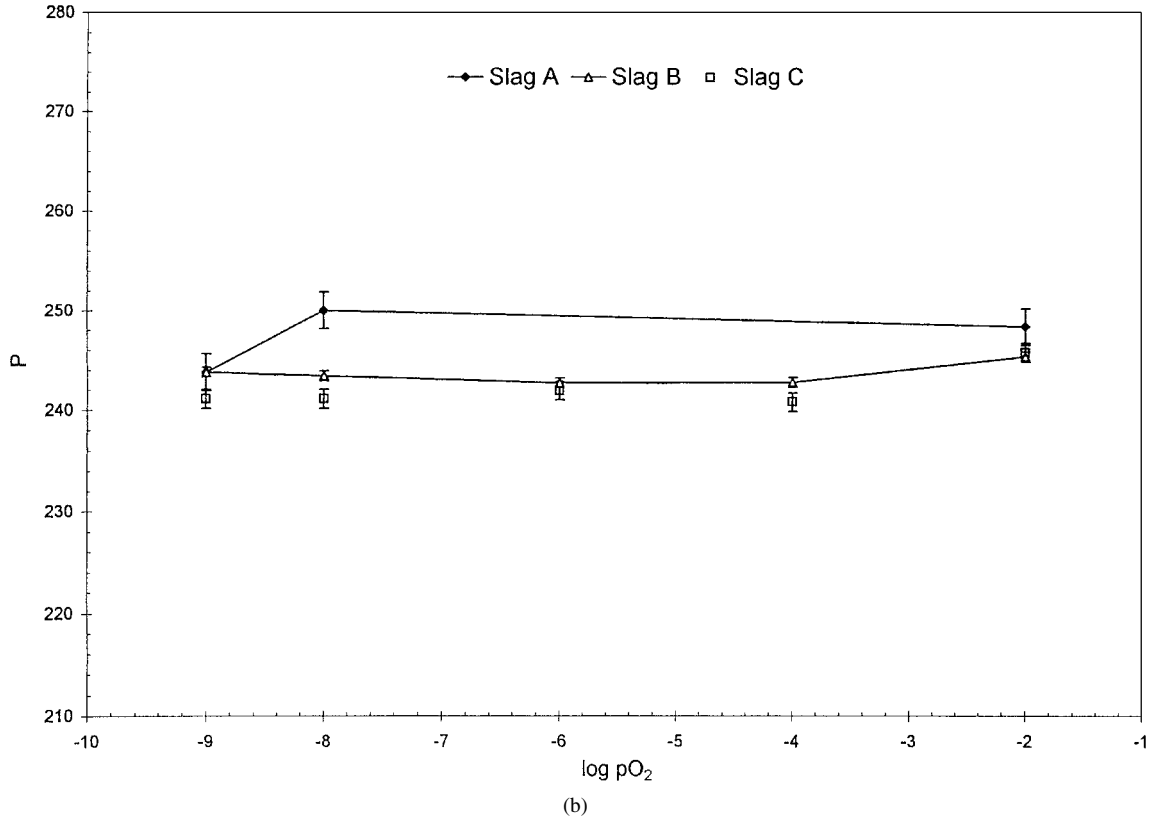

(b)

Figure 2 Variation of (a) $\Delta g_{II}/\Delta g_{\perp}$, (b) P and (c) $P\beta^2K$ with log pO_2 at different basicity ratios. (*Continued*)

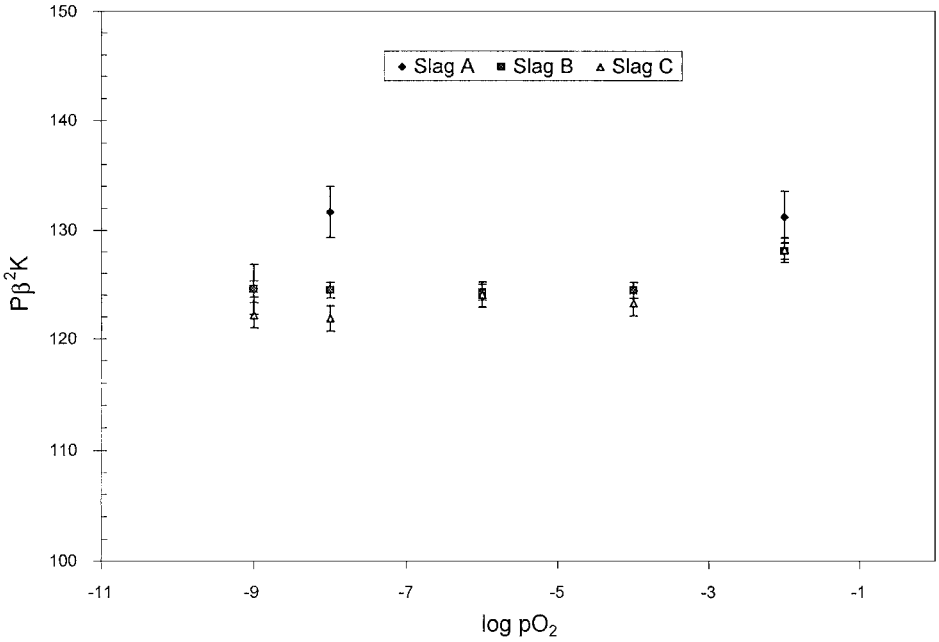

(c)

Figure 2 (*Continued*).

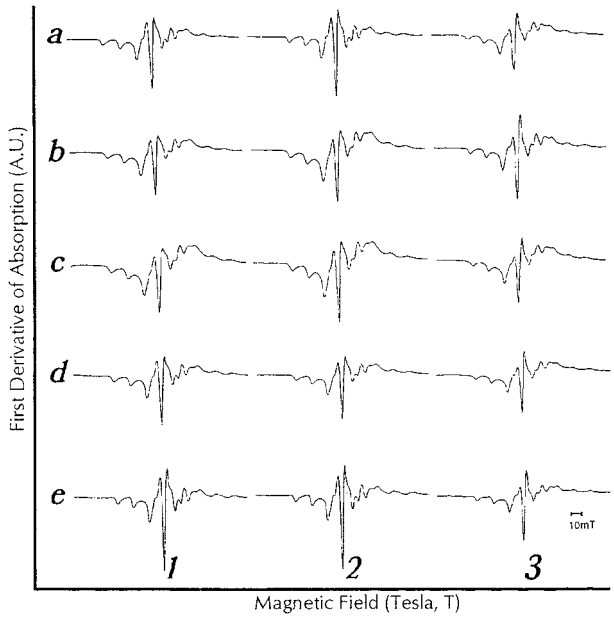

Figure 3 V^{4+} ESR spectra for quenched samples ($CaO\text{-}SiO_2\text{-}V_2O_5$ system) (1) D1–D5 $CaO/SiO_2 = 0.7$, $V_2O_5 = 1$ mol%; (2) E1–E5 $CaO/SiO_2 = 0.9$, $V_2O_5 = 1$ mol%; (3) F1–F5 $CaO/SiO_2 = 1.21$, $V_2O_5 = 3$ mol%; (1–5 in Table II is labelled a–e here). See Table I and II for details.

found at oxygen potentials between 10^{-2}–10^{-6} atm and only V^{3+}/V^{4+} pair between 10^{-8}–10^{-9} atm [8].

$\Delta g_{II}/\Delta g_{\perp}$ did not reflect any change at two levels of MgO with a variation in oxygen pressure from 10^{-2} to 10^{-6} atm (Fig. 7a). P remained constant and $P\beta^2K$ showed a slight increase from 10^{-2} to 10^{-6} atm (Fig. 7b). However the trends in bonding parameters over the whole range of oxygen pressures could not be observed due to poor resolution of the spectra below 10^{-6} atm.

The V^{4+} spectra for samples (slag H) equilibrated with an Ar-O_2(2%) gas mixture between 1–5 hours are given in Fig. 5, sequence 2. It indicates that these are similar to each other except the intensity, which is higher for one and two hours. The slag also needed greater than four hours to achieve equilibrium. $\Delta g_{II}/\Delta g_{\perp}$ did not reflect clear trends and P and $P\beta^2K$ remained same with respect to time (Table III).

3.3. $CaO\text{-}Al_2O_3\text{-}SiO_2\text{-}V_2O_5$ melt

In these slags containing 5 mol% V_2O_5 at a basicity ratio ~1.22, V^{4+} spectra followed the same pattern as for the base system (basicity = 1.23) discussed in Section (3.1) despite three different alumina contents (Table I) were used (slags I–K). The spectra for these slags (Fig. 8 sequence 1, 2, 3) started to broaden at oxygen potential 10^{-2} till 10^{-8} atm and well resolved spectra were obtained at 10^{-9} atm only. The second form of V^{4+} was dominant at oxygen pressures between 10^{4}–10^{-8} atm. The fraction of paramagnetic vanadium remained similar despite the addition of different alumina content between 3–8 wt% (Table II) over the given range of oxygen pressures. For slags I–K, only V^{4+}/V^{5+} ion pair was found at oxygen potential = 10^{-2} atm and only V^{3+}/V^{4+} pair between 10^{-8}–10^{-9} atm with an overlap of two pairs between 10^{-4}–10^{-6} atm [8].

$\Delta g_{II}/\Delta g_{\perp}$ did not indicate the clear trends within the alumina content range studied (Fig. 9a). P and $P\beta^2K$ remained same at three levels of alumina (Fig. 9b and c).

3.4. $CaO\text{-}SiO_2\text{-}V_2O_5\text{-}Fe_2O_3$ melt

Slag L and M containing high levels of V_2O_5 (10 mol%) and Fe_2O_3 (10 mol%) were melted in air. Only a broad line was obtained at two different basicity ratios. This may be attributed to the high iron content of these slags as the Fe^{3+} obscures V^{4+} because of the partial

overlapping of V^{4+} and Fe^{3+} signal which has been reported in iron bearing melts [12]. The V^{4+} content could not be measured due to the overlapping of ESR signals from Fe^{3+}.

Similarly the ESR spectrum of the industrial slag sample (from New Zealand Steel) presented a broad signal. The presence of other transition metals obscured the vanadium(IV) spectrum and only Mn^{2+} signal could be seen from the spectrum. As stated above, iron could also overlap the vanadium spectra as one of iron(III) absorption lines has the g value $\sim$2. Therefore no ESR parameters could be determined.

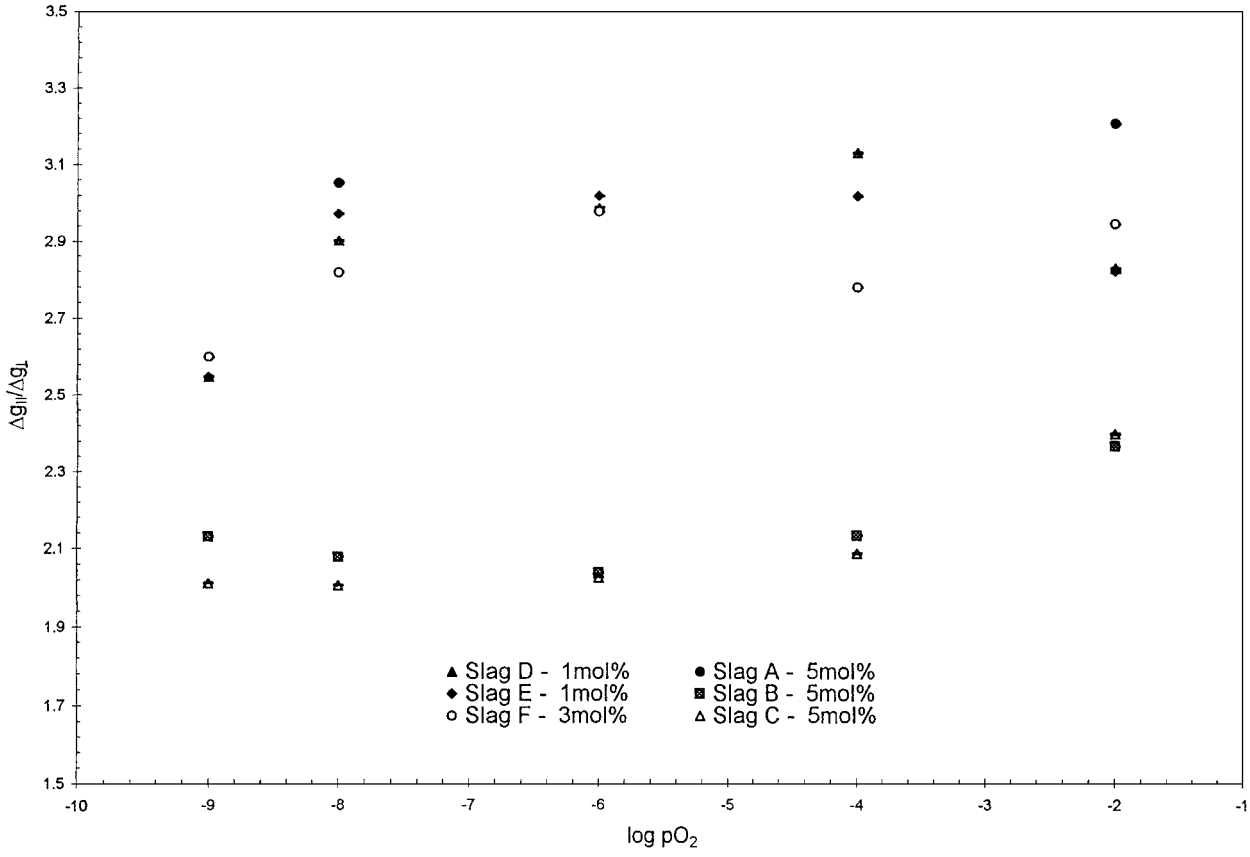

(a)

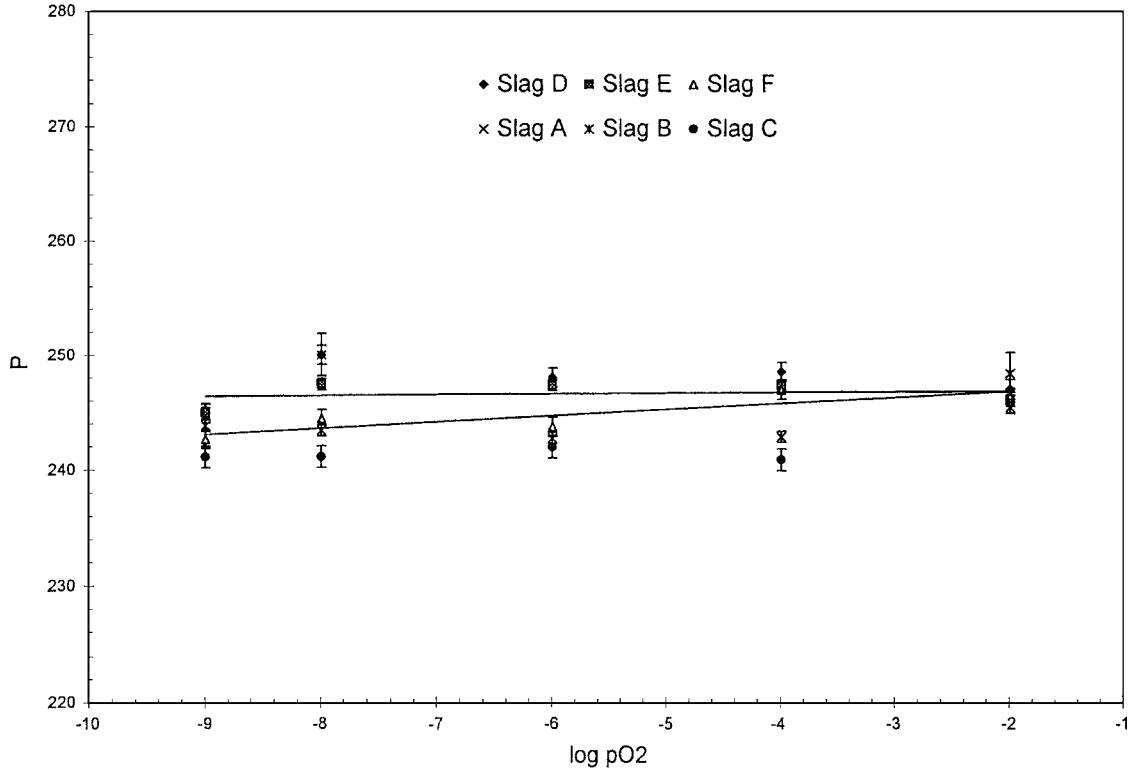

(b)

Figure 4 Variation of (a) $\Delta g_{II}/\Delta g_{\perp}$ (b) P and (c) $P\beta^2K$ with log pO_2 at different V_2O_5 contents. (*Continued*)

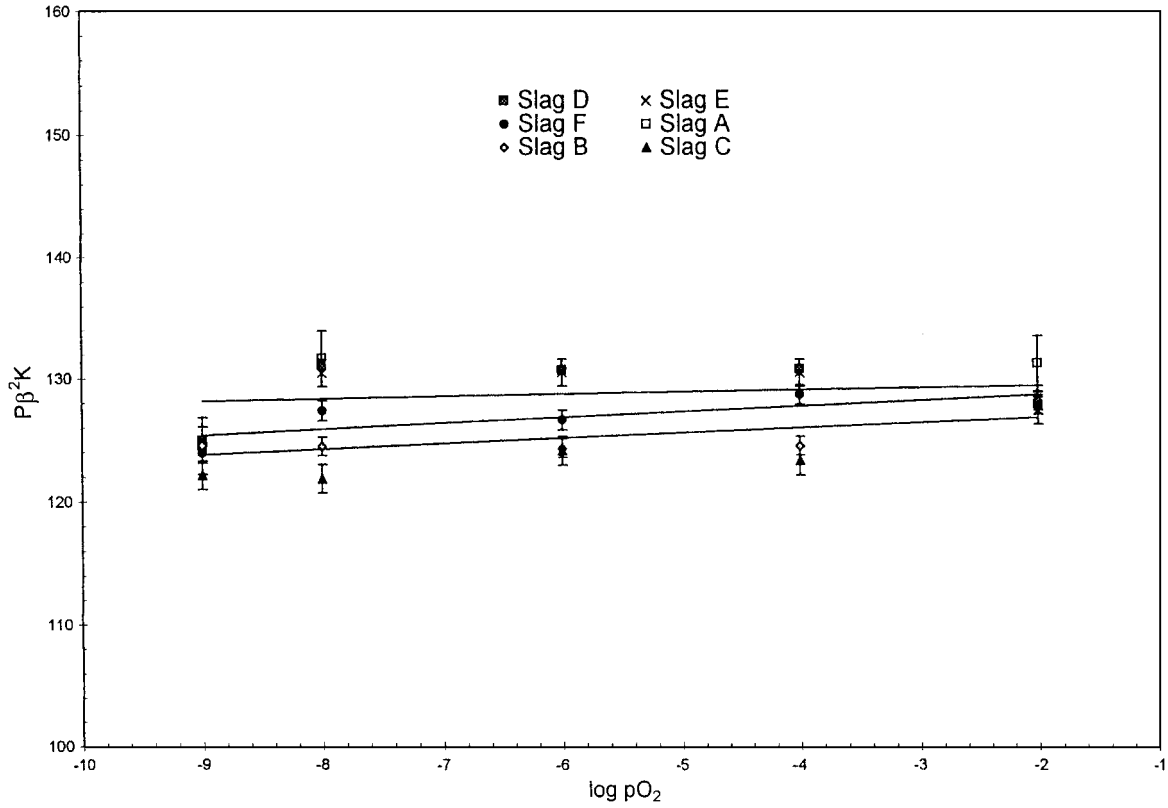

(c)

Figure 4 (*Continued*).

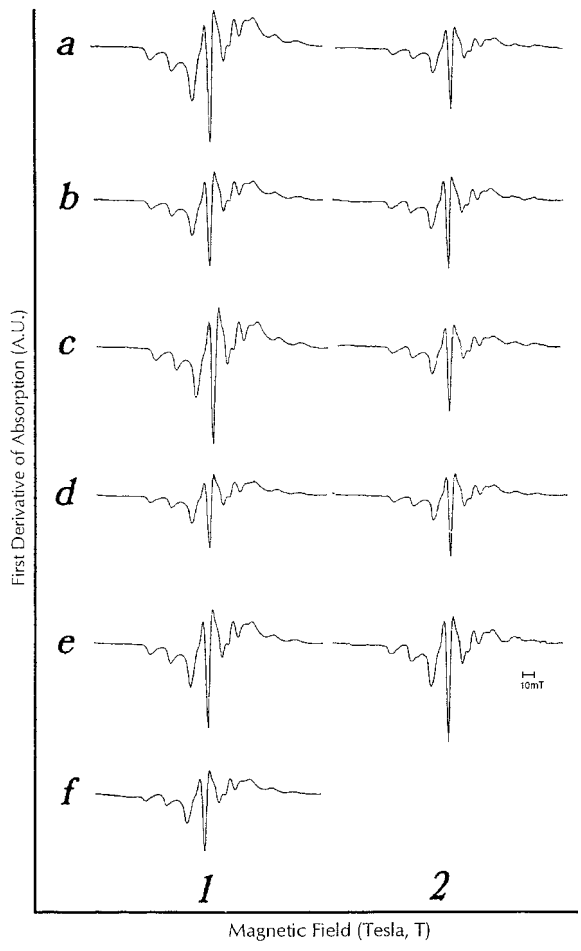

Figure 5 V^{4+} ESR spectra as function of melting time for quenched samples (1) C a–C f ($CaO\text{-}SiO_2\text{-}V_2O_5$ system, $CaO/SiO_2 = 1.23$) and (2) Ha-He ($CaO\text{-}SiO_2\text{-}MgO\text{-}V_2O_5$ system, $CaO/SiO_2 = 1.51$). (a–f represent number of hours here). See Tables I and II for details.

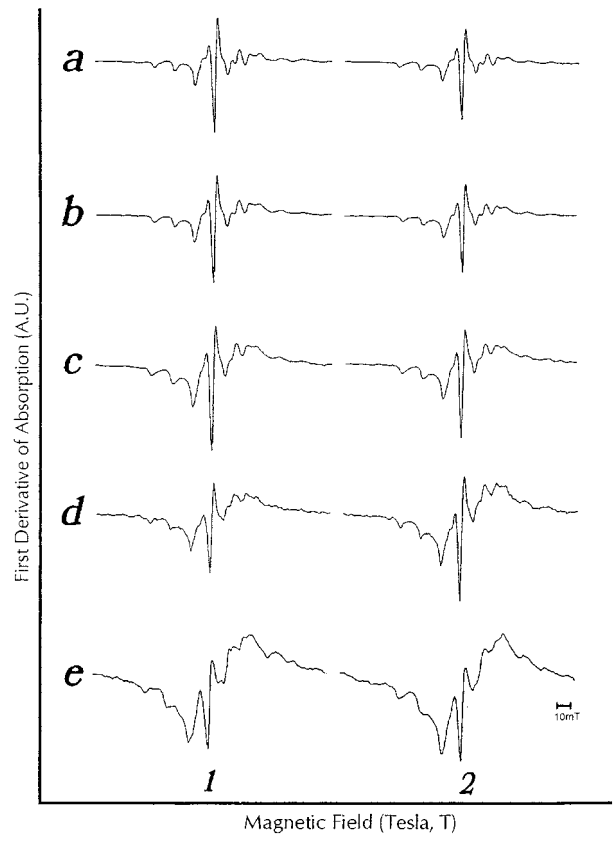

Figure 6 V^{4+} ESR spectra for quenched samples for $CaO\text{-}SiO_2\text{-}MgO\text{-}V_2O_5$ system (1) G1–G5, MgO = 3.5 wt%, (2) H1–H5, MgO = 4.87 wt%, (1–5 in Table II is labelled a–e here). See Tables I and II for details.

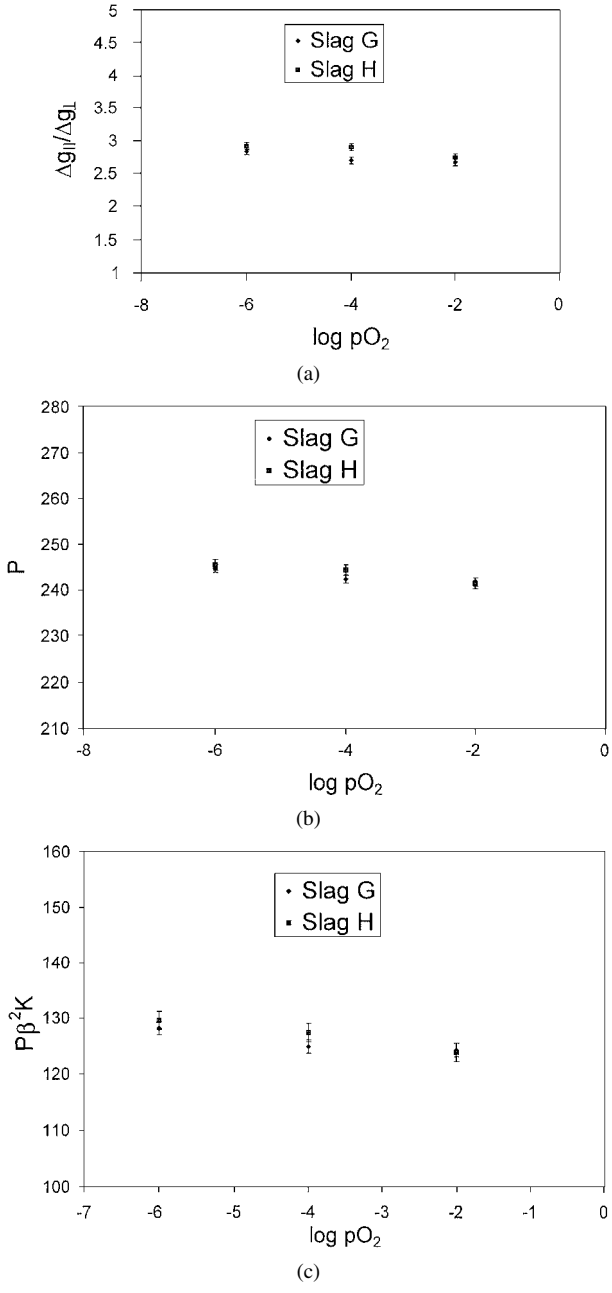

Figure 7 Variation of (a) $\Delta g_{II}/\Delta g_{\perp}$, (b) P and (c) $P\beta^2K$ with log pO_2 at different magnesia contents. Slag G, MgO = 3.5 wt% and Slag H, MgO = 4.87 wt%.

3.5. Optical properties of melts

A variety of colours were obtained for different slags although most of these were difficult to study by optical transmission due to very strong absorption. The colours of different slags are given in Table III. The important observation was the change in colour with respect to oxygen pressures. Colour changes are probably due to differences in the amount of various vanadium ions at various oxygen pressures, as well as the total vanadium content in each of these slags.

XPS spectra of slag C were recorded. However vanadium signal suffered interference from an overlapping oxygen signal (O_{1S}) in these samples. The shift in binding energies of the $V2P_{3/2}$ photoelectron peak with the change in the content of basic oxide can provide evidence of change in valence state of vanadium.

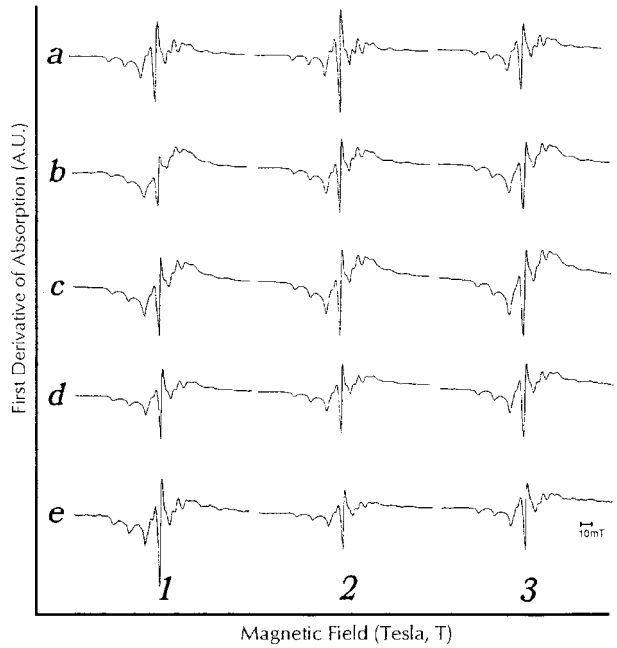

Figure 8 V^{4+} ESR spectra for quenched samples for CaO-SiO_2-Al_2O_3-V_2O_5 system (1) I1–I5 with 3.22 wt% Al_2O_3; (2) J1–J5 with 5.44 wt% Al_2O_3; (3) K1–K5 with 7.87 wt% Al_2O_3; (1–5 in Table II is labelled a–e here). See Tables I and II for details.

4. Discussion

It has been found that V^{4+} is present as VO^{2+} ion in tetragonally distorted octahedral coordination in the present slags, however a second form of vanadium(IV) also appeared. This is similar to the results from the sodium silicates [8]. Although tetrahedral V^{4+} alone has been found in some glasses previously [3, 4, 7], the second form is unidentified in that it has the same g value and overlaps the VO^{2+} spectrum in all slags investigated. This second form dominated the ESR spectra in all the present slags and over a broad range of experimental parameters. It is surprising in that it was present only under reduced oxygen pressures and high V_2O_5 content in acidic sodium silicates. Most of the current slags are highly basic in nature and prepared at high temperature (1873 K) compared to the sodium silicates, which were melted at $\leq$1598 K. The differences in the proportion of the second form of paramagnetic vanadium can be attributed to difference in composition and melting temperature.

The signals of the two forms of the paramagnetic vanadium could not be separated from the ESR measurements carried out at room temperature. The effect of the presence of the three vanadium species on the second form is not evident since the additional signal appears over nearly the whole range of oxygen pressure investigated while the three vanadium ions coexisted over a limited range of the experimental oxygen pressures (10^{-4}–10^{-6} atm). However the oxygen pressures region where the second form was present, is expanded (between 10^{-2}–10^{-8} atm) depending upon the composition of the slags. When the degree of tetragonal distortion of VO^{2+} ion decreases under reduced pressures, it may be due to diminishing of second form of paramagnetic vanadium, specifically depending on slag composition.

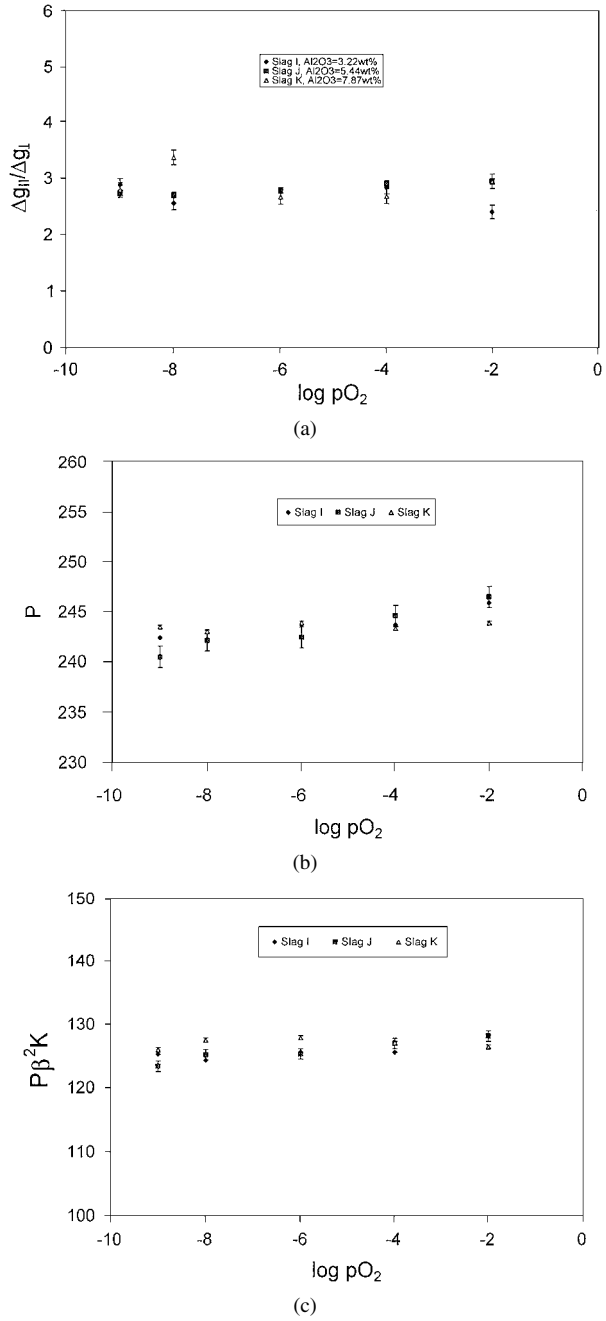

Figure 9 Variation of (a) $\Delta g_{II}/\Delta g_{\perp}$, (b) P and (c) $P\beta^2K$ with log pO_2 at different alumina contents.

The second form of the paramagnetic vanadium indicates the presence of another site, possibly a tetrahedral geometry. Bogomolova *et al.* [4] examined V^{4+} in silica glasses containing $\leq$0.5 wt% VO_2. They observed the V^{4+} in tetrahedral site while carrying the ESR measurements at 77 K. Fritsch *et al.* [7] also found V^{4+} in tetrahedral site in silica glass when spectra were recorded at $\leq$80 K. Signal broadening and overlapping have also been reported when measurements were carried at room temperature. Given that the ESR spectra of the melts in present investigation are measured at room temperature, it is possible that the second signal may be that of a tetrahedral V^{4+} ion which could not be separated from that of the VO^{2+} ion at room temperature. This indicates that the V^{4+} may be incorporated into two different sites simultaneously as reported for other transition ions, i.e. iron, [13–16]. It may only be a tetrahedral site with a background signal as shown earlier [4, 7].

4.1. Effect of basicity

As stated earlier [8], VO^{2+} ions tend to become more distorted due to the decrease in number of free O^{2-} ion or non-bridging oxygen at low basicity of the slag. The octahedral geometry of VO^{2+} is compressed due to strong bonding between V^{4+}-O_{axial}, which is outside the network. The availability of non-bridging O^{2-} with increasing melt basicity removes the stress on V-Oa bond, producing a change in structure of VO^{2+} ion as indicated by $\Delta g_{II}/\Delta g_{\perp}$ values. As discussed in Section 3.1, from the ESR spectra, the V^{4+} has been found as a distorted octahedral $(VO)^{2+}$ complex, which becomes more regularly octahedral when slag basicity is increased (Slag C, basicity = 1.23). This is in accordance with the results on sodium silicates, indicating that the V^{4+} acts as a network breaker under these conditions [8]. The addition of magnesia has a pronounced effect on the vanadyl ion since it diminishes the second form, thus favouring the octahedral coordination and network breaker role of the paramagnetic vanadium.

The amphoteric nature of alumina is obvious since there is no change in the observed vanadium coordination in the slags, at different levels of alumina investigated. This is in accord with previous work on alkali phosphate glasses where no change in the covalency of vanadium was observed with the addition of alumina [1].

There are several factors, which may be responsible for the observed changes in the coordination, i.e., more than one coordination sites for the same ion, experimental conditions, clustering.

It has been shown [17, 18] that both Fe^{2+} and Fe^{3+} ions are octahedrally coordinated at low concentration of iron in sodium and calcium silicates. Fe^{3+} adopts a tetrahedral geometry as the total iron increases. The concentration of Fe^{3+} also increases with an increase in the total iron. Proportion of the tetrahedral Fe^{3+}, which is a network former, decreases with an increase in temperature, which shows breakup of the network upon raising the temperature. The present results are in agreement with the above observations in that the octahedral coordination (network breaker) of the V^{4+} increased as the temperature was raised from 1125 to 1325°C [8] indicating a depolymerisation of the network. Accordingly, an increase in melts basicity and/or oxidised atmospheres favours the octahedral geometry of V^{4+} or network breakage.

5. Conclusions

The results of ESR study of vanadium(IV) in different metallurgical slags carried out over a range of composition and oxygen partial pressures are consistent with our previous work on sodium and calcium silicates [8, 19, 20] and others [1, 2, 5, 6, 10, 21]. The paramagnetic vanadium found was V^{4+} as the VO^{2+} ion in a tetragonally distorted octahedral site and a second form of paramagnetic vanadium was also predominantly present when the V_2O_5 and Al_2O_3 content were

increased, oxygen partial pressures was varied between 10^{-2}–10^{-8} atm and/or basicity was lowered. The second form of paramagnetic vanadium was diminished between 10^{-2}–10^{-6} atm when the MgO was added irrespective of the fraction of paramagnetic vanadium (V_{PAR}). The critical fraction for the induction of second form of paramagnetic vanadium varied with the melt composition.

The $\Delta g_{II}/\Delta g_{\perp}$ ratios are lowered under reduced oxygen pressures and with an increase in basicity indicating a more regular octahedral geometry. The decrease in P and $P\beta^2K$ values with an increase in basicity shows a decrease in covalency and the tetragonal distortion. $\Delta g_{II}/\Delta g_{\perp}$, P and $P\beta^2K$ values remained independent of the alumina content investigated. The V_2O_5 concentration range studied was not sufficient to change the covalency of vanadium.

Acknowledgment

The author gratefully acknowledges the financial support for this project from BHP Research, Center for Metallurgy and Resource Processing, Newcastle, Australia.

References

1. A. PAUL and F. ASSABGHY, *J. Mater. Sci.* **10** (1975) 613.
2. H. HOSONO, H. KAWAZOE and T. KANAZANA, *J. Non-Cryst. Solids* **33** (1979) 125.
3. A. GOLDSTEIN, V. CHIRIAC and D. BECHERESCU, *ibid.* **19** (1987) 271.
4. L. D. BOGOMOLOVA, A. N. KHABAROVA, E. V. KLIMASHINA, N. A. KRASIL'NIKOVA and V. A. JACHKIN, *ibid.* **103** (1988) 319.
5. R. MUNCASTER and S. PARKE, *J. Phy. Chem. Solids* **24** (1977) 399.
6. S. GUPTA, N. KHANIJO and A. MANSINGH, *J. Non-Cryst. Solids* **181** (1995) 58.
7. E. FRITSCH, F. BABONNEAU, C. SANCHEZ and G. CALAS, *ibid.* **92** (1987) 282.
8. H. FARAH, Ph.D. Dissertation, UNSW, Australia (1999) p. 74, 81, 86–106, 109, 132.
9. M. NAGANO, A. KATO, I. MOCHIDA and T. SEIYAMA, *J. Ceram. Soc. Japan* **78** (1970) 401.
10. D. PRAKASH, V. P. SETH, I. CHAND and P. CHAND, *J. Non-Cryst. Solids* **204** (1996) 46.
11. H. CHAUDARY, M. P. BRUNGS, D. M. MILLER and G. R. BELTON, in Proceedings of the 5th International Conference on Molten Slags, Salts and Fluxes, Sydney, January 1997, edited by (ISS, Warrendale, 1997) p. 493.
12. L. D. BOGOMOLOVA, M. P. GLASSOVA, S. I. DUBATOVKO, S. I. REIMAN and N. SPASIBKINA, *ibid.* **58** (1983) 71.
13. R. A. LEVY, C. H. P. LUPIS and P. A. FLINN, *Phy. Chem. Glasses* **17** (1976) 94.
14. S. WRIGHT and S. JAHANSHAHI, *I.S.I.J. Intern.* **33** (1993) 195.
15. N. IWAMOTO, Y. TSUNAWAKI, H. NAKAGAWA, T. YOSHIMURA and N. WAKABAYASHI, *J. Non-Cryst. Solids* **29** (1978) 347.
16. L. PARGAMIN, C. H. P. LUPIS and P. A. FLINN, *Met. Trans.* B **3** (1972) 2093.
17. C. M. BRODBECK, *J. Non-Cryst. Solids* **40** (1980) 305.
18. B. HANNOYER, M. LENGLET, J. DURR and R. J. CORTES, *ibid.* **151** (1992) 209.
19. H. CHAUDARY, M. P. BRUNGS and G. R. BELTON, in Proceedings of the 2nd Australian Melt Chemistry Symposium, Melbourne, February 1995, edited by Steven Wright (CSIRO, Melbourne, 1995) p. 25.
20. H. CHAUDARY, M. P. BRUNGS, D. M. MILLER and G. R. BELTON, in Proceedings of the 3rd Australian Melt Chemistry Symposium, Melbourne, January 1996, edited by Steven Wright (CSIRO, Melbourne, 1996) p. 169.
21. R. V. ANAVEKAR, N. DEVRAJ, K. P. RAMESH and J. RAMAKRISHNA, *Phys. Chem. Glasses* **33** (1992) 116.

Received 11 March
and accepted 31 October 2002